NMR WETTABILITY INDEX MEASUREMENTS AND METHODS COMPARED ON A VARIETY OF UNCONVENTIONAL SAMPLES

Shaina Kelly[1], Ron J. M. Bonnie[1], Michael J. Dick[2], Dragan Veselinovic[2]

[1]*ConocoPhillips Company, Houston, TX* [2]*Green Imaging Technologies, Fredericton, NB, Canada*

This paper was prepared for the SPWLA 62nd Annual Logging Symposium held online from May 17-20, 2021.

ABSTRACT

Matrix wettability is a key driver in relative permeability and, hence, a critical factor controlling imbibition and drainage at UR fracture-matrix interfaces as well as enhanced oil recovery (EOR). In this study, we (1) adapt and apply the NMR-based wettability index (NWI) methodology of Looyestijn et al. (2006) to a variety of unconventional twin samples undergoing, respectively, spontaneous imbibition with oil-displacing-water and water-displacing-oil and (2) compare the robustness of this method among a variety of samples pairs and also to other NMR-based wettability methods. The samples analyzed cover a range of rock types, major formations, maturity and content of organic material. All displayed unique time-lapse wettability profiles and steady state NWI values. This work advances our previous works (Dick et al., 2019; Kelly et al., 2020) on this subject, where the viability of the methodology was established on end-member pilot samples, towards applicability as a UR SCAL method.

The NWI methodology predicts T_2 spectra using linear combinations (mixing) of "end-point" T_2 spectra. The mixing ratios yielding the closest match to the measured spectra are then used to compute a wettability index. These mixing ratios were validated against (1) mass-balance calculations, (2) repeat experiments with heavy water (D_2O) instead of H_2O and (3) measured T_1-T_2 maps, enhancing confidence in the robustness of the method. Our comparisons show that alternative approaches representing the T_2 spectra through a single mean T_2 value or T_2 peak-fit, fall short, especially in tight rocks where fast relaxation rate components tend to skew harmonic mean T_2 values and also in samples where oil and water peaks are not clearly resolved. Full spectrum-based methods, akin to Looyestijn's, appear more robust and stable over a much wider range of reservoir conditions.

Repeated NMR acquisition throughout our long-term imbibition experiments shows that time-lapse NWI methodology probes the effects of rock properties, saturation changes, and injected fluid chemistry (enhanced oil recovery strategies) on wettability alteration. Additionally, this NWI study quantifies the wide variation in wettability among unconventional samples.

INTRODUCTION

Reservoir wettability factors into key unconventional petro-technical decisions related to fracture fluid additives and soaking times and dictates the relative permeability curves selections used in reservoir modeling. Wettability is a complex function of surface chemistry and adsorption and can be challenging to predict with multiple mineral surfaces, in situ brine composition uncertainty, and complex oil chemistries, all characteristics of unconventional reservoirs. Note that a thorough review of wettability fundamentals and capillary pressure for oilfield applications can be found in the work of Hirasaki (1991). Conventional wettability determination methods that yield quantitative indices by way of changes in saturations with spontaneous and forced imbibition (displacement) include the Amott and USBM methods. A review of these methods and some of their advantages and pitfalls are detailed in Morrow et al. (1994). There currently is no industry established wettability evaluation methodology for UR.

In the past decade (plus), NMR has moved from "niche" to "main-stream" and is often a critical tool in laboratory core analysis and well logging programs. Rise in unconventional reservoir exploration and production has led to an increase in NMR-based core analysis methods and applications, often extensions or adaptations of proven and widely accepted methods used on conventional samples. Following this meta, we have applied the NMR-based wettability index (NWI) determination technique (Looyestijn and Hofman, 2005; Looyestijn et al., 2017) to "geological twin" samples from various North American unconventional reservoirs and rock types. **Table 1** showcases the variety of samples and some of their attributes relevant to this study. All of the samples were approximately 2.5 cm in diameter and 4-5 cm in length. Some of the samples (the 7-P, 2-P, and GP sets) were analyzed in our previous works (Kelly et al., 2020) on NMR-based wettability, where the viability

Table 1: Core Plug Sample Information

Rock Type	Reservoir ID	Sample Name*	Original State+	Helium Porosity (%)	MICP Porosity (%)	LECO TOC (wt%)	XRD Mineralogy (wt%)
Marl (high maturity)	A	9-P1A	100% Decane Saturated	10.3	10.8	5.07	Quartz: 15.2 Feldspar: 4.3 Carbonate: 51.9 Total clay: 23.6 Pyrite: 4.1 Marcasite: 0.9
		9-P3	100% Brine (4% NaCl) Saturated				
Marl (low maturity)	A	7-P2	100% Brine (4% NaCl) Saturated	12.5	12	4.38	Quartz: 21.1 Feldspar: 3.9 Carbonate: 46.5 Total clay: 23.4 Pyrite: 4.6 Marcasite: 0.6
		7-P3A	100% Decane Saturated				
Marl	D	12-1	100% Decane Saturated	4.6-6.3	---	3.27-4.54	Quartz: 9 Feldspar: 2 Carbonate: 74 Total clay: 12 Pyrite: 3
		12-6	100% Brine (4% NaCl) Saturated				
Chalk	D	14-1	100% Decane Saturated	6.6-7.2	---	1.16-2.85	Quartz: 5 Feldspar: 1 Carbonate: 89 Total clay: 4 Pyrite: 1
		14-7	100% Brine (4% NaCl) Saturated				
Chalk	B	2-P2	100% Brine (4% NaCl) Saturated	4.3	4.1	0.39	Quartz: 3.8 Feldspar: 2.3 Carbonate: 85 Total clay: 6.6 Pyrite: 1 Marcasite: 0.7
		2-P1A	100% Decane Saturated				
Siltstone	C	GP2	100% Brine (9% NaCl) Saturated	8.8	8.4	1.89	Quartz: 67.9 Feldspar/ Plagioclase: 6.7 Carbonate: 2.8 Total clay: 14.3 Pyrite: 5.8 Marcasite: 1.6
		GP3	100% Decane Saturated				

*Samples for each rock types are twins from the same depth station. The reservoir D plugs were offset at the sampling station, rendering a range in values, as shown in the table.
***Approximate* steady-state value from convergence of curves from both twin samples
+ Brine concentrations replicated the corresponding estimated values for formation connate water

of the methodology (Dick et al., 2019) was established on end-member pilot samples. We encourage the reader to review those findings. This work extends the method to a larger variety of rock types, some rendering challenging spectra, to establish the applicability of the NWI as a wettability evaluation methodology for UR (SCAL method); method limitations are discussed as well.

The NWI measurement methodology utilized on tight rocks in this study provides a quantitative wettability value for comparison among rock samples and varied states: 0.3 to 1 = water wet, -0.3 to 0.3 = mixed wet, and -0.3 to -1 = oil wet. During spontaneous imbibition of fully saturated samples (various fluid combinations) temporal changes in saturations and a quantitative wettability index are determined, as detailed in the subsequent sections.

Finally, note that the samples, even when preserved via wrapping and sealing procedures, are not "fresh" core plug samples in that the corresponding wells were drilled several years ago. In addition, the sample workflows are applied "as-received" with drying steps such that the samples do not undergo any cleaning procedures, which can be challenging/damaging on tight rocks. Therefore, it is possible that the wettability state of the samples may be slightly altered as compared to the reservoir state due to the residence time of dead crude oil in the plugs, drying of clays, etc. Even with this caveat, distinct NWI differences among the samples indicates pronounced differences in wetting conditions among and within UR plays.

Table 2: CPMG Sequence Acquisition Parameters

Sample	TW* (ms)	Signal to Noise Ratio	TE (µs)	Number of Echoes	NMR Porosity** (p.u.) or Volume (ml)	P90 (µs)
9P1A	750	200	50	5,000	9.5 p.u.	7.51
9P3	750	200	50	5,000	10.4 p.u.	7.51
12-1	750	200	50	5,000	1.8 p.u.	7.51
12-6	750	200	50	5,000	3.3 p.u.	7.51
14-1	750	200	50	5,000	4.9 p.u.	7.51
14-7	750	200	50	5,000	4.4 p.u.	7.51
Bulk Decane	18,750	164	50	125,000	4.69 ml	7.51
Bulk Brine	22,500	236	50	150,000	6.38 ml	7.51

*Post-sequence wait time
**NMR porosity was obtained by subtracting T_2 spectra measured on dried samples from the T_2 spectra measured at 100% Sw. Subtraction was done in time domain and then the subtracted data was inverted.

METHODS

NMR Wettability Index

Our NMR based wettability determination methodology requires T_2 spectra of both study samples and bulk-fluids. The essential acquisition parameters used in the CPMG pulse sequence yielding these T_2 spectra are summarized in **Table 2**.

The NMR-based wettability index was computed using an adaptation of Looyestijn's NWI model, which is based on the premise that the NMR T_2 spectra of oil- and brine-saturated rock samples vary in accordance to changes in the wetting conditions of the samples. One key advantage of its approach over most NMR wettability models (Fleury and Deflandre, 2003; Howard, 1998; Tandon et al., 2017; Newgord et al., 2018) is the use of T_2 spectra at any saturation level with no requirement for S_{wi} and S_{or} T_2 spectra as input. Another major advantage is its use of complete T_2 spectra rather than a single relaxation rate (usually T_2 log mean or T_2 harmonic mean) for NWI calculations. This enhances the stability and robustness of the method drastically as minor variations in T_2 spectra do not result in major changes in the NWI result, which is often seen with single T_2 value-based models. Consequently, our NWI model is well suited for data sets featuring complex oil and water T_2 spectra with multiple peaks. NWI determination using this model requires: NMR T_2 spectra of (1) 100% brine saturated sample, (2) 100% oil (decane) saturated sample, (3) bulk oil (decane) and (4) bulk brine. All saturated rock core plug T_2 data was obtained by subtracting dry (background) T_2 spectrum from (original) saturated T_2 spectra. Subtraction was done in time domain and then the subtracted data was inverted. A linear combination of these 4 input spectra constitutes a predicted T_2 spectrum (S_{pred}) for the oil and brine saturated sample which is subsequently compared to the actual / measured spectrum (S_{mix}). The relative strength or contribution of each component / input spectrum is established through least squares optimization, establishing representative mixing functions H and W:

$$H = \frac{a_1 - a_2}{1+\left(\frac{r}{r_a}\right)^{\alpha}} + a_2,\ W = \frac{b_1 - b_2}{1+\left(\frac{r}{r_b}\right)^{\beta}} + b_2 \qquad (1)$$

H describes the fraction of pores occupied by water and W describes the fraction of pores wetted by water. We can greatly simplify Eq.1 as in our implementation of the model, $a_1 = b_1 = 1$, $a_2 = b_2 = 0$ and $\alpha = \beta = 2$. Finally, the pore size radius, *r*, is substituted by T_2 since pore size radius is proportional to transverse relaxation time T_2.

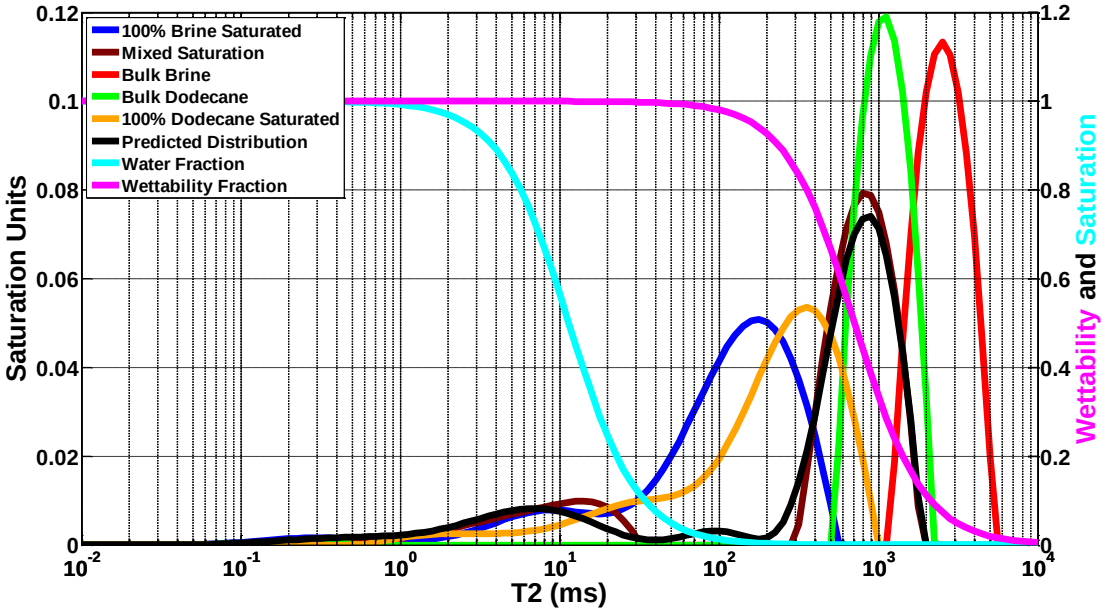

Figure 1: Typical bulk-T_2 spectra used for wettability determination (left axis). The water fraction (light blue) and wettability fraction (pink) are also shown (right axis). This data is for instructional purposes only was not recorded as part of this investigation of wettability of unconventional samples.

With that, Eq. 1 can be rewritten as:

$$H = \frac{1}{1+\left(\frac{T_2}{r_a}\right)^2}, W = \frac{1}{1+\left(\frac{T_2}{r_b}\right)^2} \quad (2)$$

In **Figure 1**, we show examples of the H (light blue) and W (pink) functions. The physical interpretation of our model assumes that all pores to the left of the inflection point (i.e. 2nd derivative changing sign) on W are water wet and all pores to the right of that inflection point are oil wet. Similarly, all pores to the left of the inflection point on H are occupied by water and all pores to the right of the inflection point on H are occupied by oil. The inflection points in H and W, i.e. maximum size of pores that are both water-wet and completely filled with water, respectively, can be varied by adjusting r_a and r_b respectively.

After establishing these mixing functions, the model T_2 distribution (S_{pred}) for the mixed-saturation sample is computed according to Equation 3.

$$S_{pred} = WHS_{w-100\%} + (1-W)(1-H)S_{o-100\%} + (1-W)HS_{w-bulk} + W(1-H)S_{o-bulk} \quad (3)$$

In this equation, the four measured T_2 spectra (1) $S_{w\text{-}100\%}$, (2) $S_{o\text{-}100\%}$, (3) $S_{w\text{-}bulk}$ and (4) $S_{o\text{-}bulk}$ are weighted by the mixing functions H and W and combined to give a predicted T_2 distribution, S_{pred}. Finally, only r_a and r_b , need to be adjusted in a least squares fashion to minimize the difference between S_{mix} and S_{pred}.

The black trace in **Figure 1** shows the resulting modeled T_2 distribution based on the final H (light blue trace) and W (pink trace) functions established in the least squares fitting procedure just described. One can see the good agreement between the predicted and measured mixed-saturation T_2 distributions (brown trace).

With the final H and W functions in hand, one can quantify the saturation and wettability through Equations 4 and 5. For the data shown in **Figure 1**, this yields a Predicted Water Saturation (S_{wett}) of 0.13 and the NMR Wettability Index (NWI) is 0.89.

$$Water\ Saturation = S_{wett} = \sum_{T_2} S_{w-100\%}H \quad (4)$$

$$Wettability = NWI = 2\sum_{T_2} S_{w-100\%}W - 1 \quad (5)$$

Time-Lapse NWI Experiments

The NMR measurements for this wettability study were performed with a 2 MHz GeoSpec 2-75 spectrometer

Table 3: IR-CPMG Parameters

Sample	TW* (ms)	Signal to Noise Ratio	TE (µs)	Number of Echoes	Number of IR Steps	P90 (µs)
All samples	750	200	50	5000	30	7.61

*Post-sequence wait time

from Oxford Instruments[1]. The NMR data acquisition was done using Green Imaging Technologies' GIT Systems Advanced software package[2] and subsequent data processing and analysis were done using GIT Systems Advanced and MATLAB software. All sets of "twin" samples in the NWI study (for details, see **Table 1**) were oven-dried for seven days at 95 C in a vacuum oven. Prior to scanning in the NMR instrument, samples are weighed and wrapped in cellophane; this will allow for volumetric QC / reconciliation of the results. Baseline T_2 (CPMG) and T_1-T_2 spectra (inversion recovery (IR) -CPMG pulse sequence) of the dried samples were acquired using the parameters in **Table 2** and **Table 3**, respectively. The same parameters were used for all subsequent T_2 and T_1-T_2 measurements. The T_1-T_2 maps are not being used in NWI analysis, but these maps give an indication of which pores are oil-occupied and which pores are water-occupied.

Following the oven-drying and baseline measurements, one sample of each twin set was 100% saturated with decane while the other was 100% saturated with 4% NaCl brine. Subsequently, T_2 and T_1-T_2 spectra of these fullysaturated samples were acquired. The decane saturated samples were then placed in a brine bath, while the brine saturated samples were placed in a decane bath. As spontaneous imbibition commenced, the samples were periodically taken out of their bath, briefly rolled on to paper towel to remove excess liquid droplets on the sample surface, weighed, wrapped in cellophane and scanned in the NMR spectrometer. Upon completion of the NMR measurements, the cellophane was removed again, and samples were placed back into their respective baths. This process continued until imbibition equilibrium was reached (i.e., NMR T_2 data stopped changing). For some samples, the time to reach equilibrium was on the order of 100 days, for others it took only a few weeks.

Once equilibrium was reached in the spontaneous imbibition experiment, samples were oven dried again and saturated with the "opposite" fluids from the previous experiment (decane to brine and vice versa). NMR- and weight data was again acquired on these re-saturated samples. This final step completes acquisition of all data required for a proper NWI analysis. At this stage, we also compare the T_2 distributions for the twins at 100% S_w and 100% S_o respectively. It was noted that these endpoint spectra are sometimes slightly different, likely due to thin-bedded nature of these reservoirs (heterogeneity) and sampling offset between plugs taken from the same general core station. Samples 12-1/12-6 and 14-1/14-7 were the pairs with the, respectively, greatest offsets in sampling distance and T_2 endpoint spectra.

To validate the NWI method, we dried the samples and saturated them with brine and decane once again, as in the initial experiment. This time, however, we used deuterated (heavy water, D_2O) based brine instead of the regular 4% NaCl brine. We are leveraging the fact that D_2O behaves chemically no different than H_2O yet is physically different and exhibits no NMR signature; hence, during the measurement, the NMR spectrometer will only record signal from the hydrogen atoms in the decane. This D_2O benchmarking is very helpful as it allows us to determine accurate saturation at any point during the imbibition experiment. This saturation can then be used to check the NWI model saturation independently or to ground the saturation when using the model. The rest of the D_2O experiment is identical to the initial experiment.

RESULTS

In this section we detail the time-lapse NWI results from the spontaneous imbibition experiments. The subsequent subsections showcase the dynamic data set and **Table 4**

[1] Geo-Spec 2-75 User Manual, Version 1.8, Oxford Instruments.

[2] GIT Systems and LithoMetrix User Manual, Revision 1.9, Green Imaging Technologies

in the Discussion section summarizes the end-point values (steady state). The decane-brine data is overlain with the decane-D_2O validation data sets and the mass-balance calculations and T_1-T_2 maps are integrated in the last two subsections for additional benchmarking support. Again, for the 7-P, 2-P, and GP sample sets we encourage the reader to review the findings in our previous work (Kelly et al., 2020), presented in a similar format.

Samples 9-P

Figure 2 shows the results of the wettability analysis for twin samples 9-P1A and 9-P3A. **Table 1** shows the original state of each twin prior to the initiation of the imbibition experiment. The left-hand panel of **Figure 2** displays the wettability as a function of imbibition time for both samples, while the right-hand panel of **Figure 2** shows the water saturation as a function of imbibition time for both samples. Looking at the wettability change for twin 9-P1A (**Figure 2** – left panel – blue trace), it is observed that the rock started in an oil wet state but changed to mixed wet over the first two weeks of brine imbibition. The NMR wettability index then stabilized between -0.2 and 0 for the remainder of the imbibition study. The shape of the brine saturation vs elapsed time curve for twin 9-P1A (**Figure 2** – right panel – blue trace) mirrored the change in wettability for this sample. It increased from 0% to around 40% by day fifteen where it remained stable for the remainder of the experiment. The wettability and saturation levels for sample 9-P3A are also shown in the left and right panels of **Figure 2**. Looking at the wettability change for twin 9-P3A (**Figure 2** – left panel – red trace), it is observed that the rock started out water wet but quickly became mixed wet by day fifteen of the experiment. The sample remained mixed wet for the remainder of the experiment. The brine saturation vs. elapsed time for twin 9-P3A showed a similar rapid decrease as the wettability. The sample started out at 100% brine saturated but quickly dropped to near 50% brine saturated by day fifteen. Following this initial decrease in brine saturation for sample 9-P3A, its brine saturation seemed to increase slightly over the remainder of the experiment. Clearly it is not physically possible for a rock imbibing decane to have its brine saturation increase over time. The slight increase in brine saturation observed after day fifteen for sample 9-P3A is likely a result of anomalies in the wettability analysis.

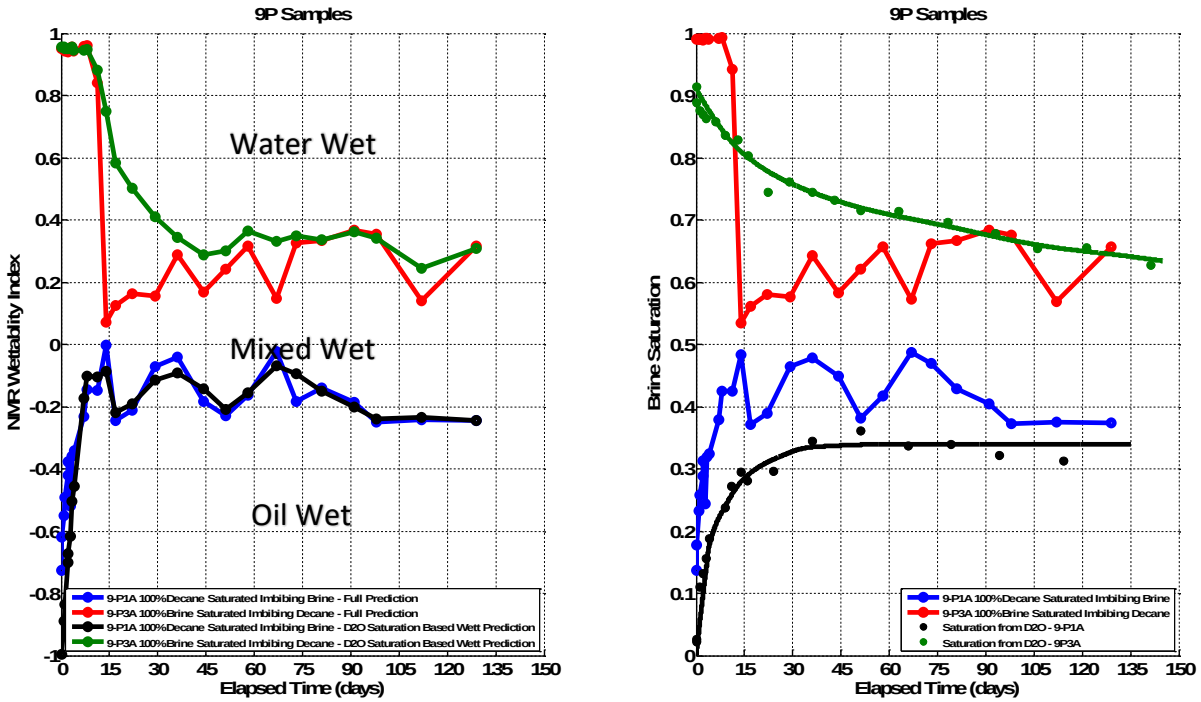

Figure 2: The results of the wettability analyses for twins 9-P1A and 9-P3A are shown. The left-hand panel shows the wettability as a function of imbibition time for both samples, while the right-hand panel shows the water saturation as a function of imbibition time for both samples.

The D_2O imbibition data was employed to confirm the validity of the results of the wettability analysis. The green and black traces in the right panel of **Figure 2** show the brine saturation measured by D_2O for samples 9-P3A and 9-P1A respectively. For sample 9-P1A, the saturation measured from the D_2O data (**Figure 2** – right panel – black trace) agrees well with the predicted saturation (**Figure 2** – right panel – blue trace). This is especially true after day one hundred where both the predicted and D_2O based brine saturations stabilize near 35%. For sample 9-P3A, the D_2O based saturation data (**Figure 2** – right panel – green trace) shows that the brine saturation changes slower than the NWI-based saturation (**Figure 2** – right panel – red trace). However, by day seventy-five there is excellent agreement between the predicted and D_2O based brine saturations. The D_2O data also shows that the brine saturation is not increasing slowly with time after day fifteen. This further confirms the assumption that the slight increase of brine saturation with time observed for sample 9-P3A is in fact due to anomalies of the NWI prediction.

Finally, the wettability analysis was repeated with the saturation fixed at the D_2O-based saturation values. The result was a new NWI versus elapsed time analysis for both the 9-P1A and 9-P3A samples. These plots were compared with the predicted wettability versus elapsed time plots to see what effect any discrepancy between predicted and D_2O-based saturations would have on the predicted wettability. For 9-P1A, there was excellent agreement between the wettability predicted from the NMR analysis (**Figure 2** – left panel – blue trace) and that retrieved with the saturation fixed at the D_2O based saturations (**Figure 2** – left panel – black trace). For sample 9-P3A, there was also good agreement between the wettability predicted from the NMR analysis (**Figure 2** – left panel – red trace) and that retrieved with the saturation fixed to the D_2O based saturations (**Figure 2** – left panel – green trace). The D_2O based wettability showed a slightly slower change of the wettability for sample 9-P3A from water wet to mixed wet. This is unsurprising as the D_2O saturation data showed a slower change in saturation versus elapsed time than predicted by the wettability analysis.

Samples 12

Figure 3 shows the results of the wettability analysis for sample 12-1. As summarized in **Table 1**, originally twin samples were prepared for study, one 100% decane saturated and the other 100% brine saturated. However, during the study the 100% decane saturated twin split rendering it useless for study. The left panel of **Figure 3** displays the predicted wettability as a function of imbibition time for sample 12-1 (red trace) which began as 100% brine saturated and was imbibing decane. The wettability began near 0.8 and was steadily decreasing for the first twenty days. After day twenty, the wettability dropped quickly to approximately 0.1 where it remained stable for the remainder of the experiment. The right panel of **Figure 3** shows the predicted brine saturation (red trace) as a function of elapsed time for sample 12-1. The brine saturation dropped steadily for the first twenty days before stabilizing near 55%.

The imbibition study was again repeated with D_2O to validate the results of the NMR wettability analysis. The green trace in the right panel of **Figure 3** shows the brine saturation versus elapsed time based on the D_2O data. The D_2O based saturation began as 100% saturated and eventually stabilized near 75% brine saturated. This is nearly 20% higher than the saturation predicted by the wettability analysis (**Figure 3** – right panel – red trace). When the D_2O based saturation, data is used to predict the wettability for sample 12-1 (**Figure 3** – left panel – green trace) it stabilizes near an NWI of 0.4 after ninety days of imbibition. This is different from the stable wettability of 0.1 predicted by the NMR analysis (**Figure 3** – left panel – red trace). The discrepancy between the predicted and D_2O based wettability is a result of the NMR wettability model being pushed to the limit of its capabilities. Sample 12-1 has multi-peak 100% S_w and 100% S_o T_2 distributions and a mixed wettability, both of which increase the probability that T_2 distributions will have overlapping features which increases uncertainty in the wettability analysis. This limitation will become more obvious when the next sample is discussed.

Samples 14

Figure 4 shows the results of the wettability analysis for twin samples 14-1 and 14-7. **Table 1** shows the original state of each twin prior to the initiation of the imbibition experiments. Looking at sample 14-1, the left panel of **Figure 4** shows that NWI for this sample (blue trace) starts near -0.5 and becomes more mixed wet over time eventually stabilizing with a wettability near -0.2. The saturation predicted by the NWI analysis for sample 14-1 (**Figure 4** – right panel – blue trace) shows an increase in brine saturation over time starting at near 0% before increasing and stabilizing near 15% after ninety days. The D_2O based saturation data for sample 14-1 (**Figure 4** – right panel – black trace) shows a larger change in brine saturation over time as compared to the saturation predicted from the NWI analysis. The discrepancy

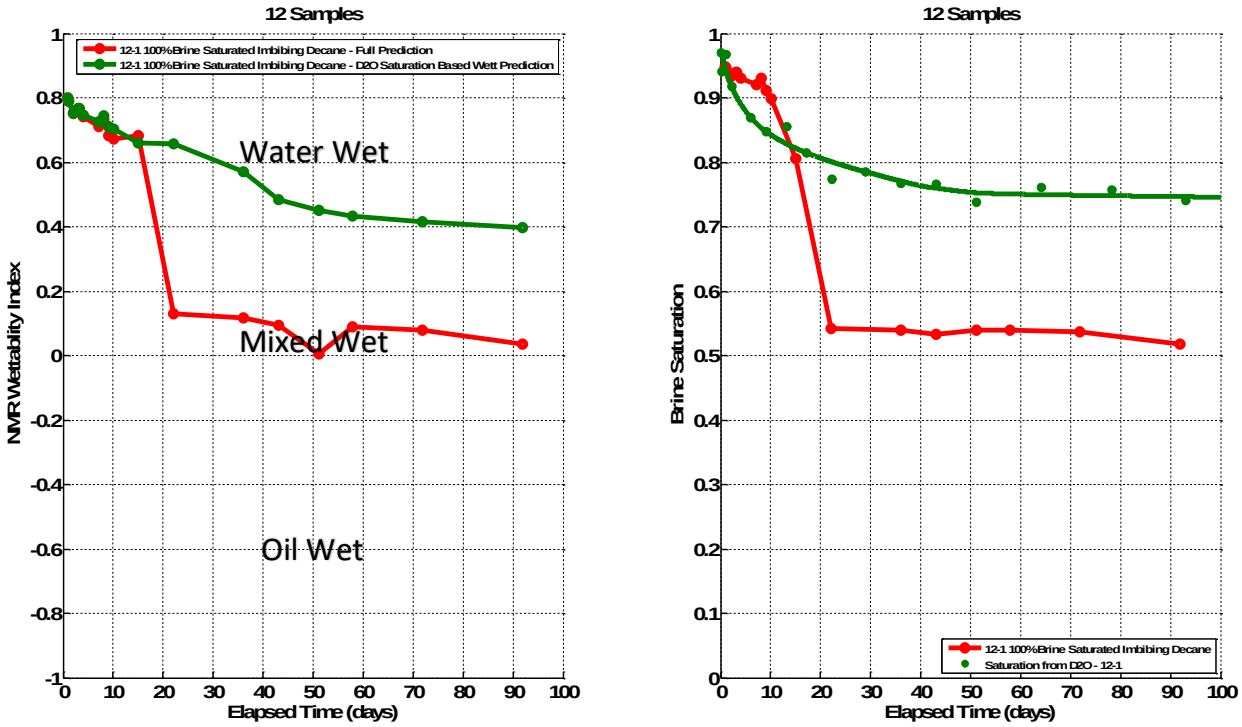

Figure 3: The results of the wettability analyses for sample 12-1 are shown. The left-hand panel shows the wettability as a function of imbibition time for both samples, while the right-hand panel shows the water saturation as a function of imbibition time for both samples. Originally twin samples were prepared for study, one 100% decane saturated and the other 100% brine saturated. However, during the study the 100% decane saturated twin split rendering it useless for study and hence the data is not plotted here.

between the predicted and D_2O based saturations can be understood looking at the left-hand panels of **Figure 5**. The upper panel shows the 100% S_w (blue trace) and 100% S_o (black trace) T_2 distributions for sample 14-1. As outlined earlier, the NMR wettability model mixes these spectra to give a predicted T_2 spectrum which is compared (via a least-squares fit) to a T_2 spectrum recorded from a sample partially saturated with both water and oil whose wettability is to be determined. In this case, the partially saturated T_2 spectrum the model is trying to match is shown by the red trace in the lower left panel of **Figure 5**. This T_2 distribution, which is comprised of two peaks, corresponds to the last data point for predicted wettability/saturation versus elapsed time for sample 14-1 (Blue traces on **Figure 4**). Comparing this distribution with the 100% S_o and 100% S_w T_2 distributions (**Figure 5** – upper left panel) it is obvious that the peak at lower T_2 values is comprised of only signal from the 100% S_w T_2 distribution. On the other hand, the peak at longer T_2 values is comprised of contributions from both the 100% S_o and 100% S_w T_2 distributions. This is where the wettability analysis begins to fail, it is impossible (without complimentary data) for the model to simultaneously determine the contribution from both the 100% S_o and 100% S_w T_2 distributions to this peak. This leads to uncertainties in the predictions of the NMR wettability analysis. Luckily, the D_2O data can provide the complimentary information needed to separate the contributions to this peak. The green trace in the lower left panel of **Figure 5** is the T_2 distribution recorded for sample 14-1 (100% decane saturated imbibing D_2O) and corresponds to the last data point recorded for D_2O imbibition of sample 14-1 (Black traces on **Figure 4**). In this spectrum, only signal from decane is observed so subtracting it from the partially saturated T_2 spectrum (**Figure 5** – lower left panel – red trace) it is easy to determine the brine and decane saturation for this partially saturated data. Once the saturations have been unambiguously determined, the wettability analysis can be repeated with the brine saturation fixed to the D_2O-determined saturation value. This leads to a new wettability value determined from the D_2O-based brine saturation (**Figure 4** – left panel – black trace). It should be noted that whenever there is disagreement between the D_2O-based saturation results and the results from the NMR wettability analysis alone, the D_2O data is taken as correct because there is unambiguity in these results.

Looking at **Figure 4**, the disagreement between the

predicted brine saturation and the D_2O based saturation for sample 14-7 is very pronounced. According to the NMR wettability analysis the saturation (**Figure 4** – right hand panel – red trace) does not change over the elapsed time of the experiment. On the other hand, the D_2O data (**Figure 4** – right panel – green trace) shows that the brine saturation drops from 100% to approximately 80% over the course of the experiment. The predicted wettability for sample 14-7 also shows no change over the course of the experiment (**Figure 4** – left hand panel – red trace) while the wettability derived with the saturation fixed to the D_2O data (**Figure 4** – left hand panel – green trace) shows a drop from near 1 to approximately 0.6 over the course of the experiment. The reason for these discrepancies is again due to the limitations of the NMR wettability analysis caused by overlapping T_2 distributions. The upper right-hand panel of **Figure 5** shows the 100% S_w (blue trace) and 100% S_o (black trace) for sample 14-7. Clearly there is significant overlap between these distributions. The lower right-hand panel of **Figure 5** shows the T_2 distribution (red trace) for the last predicted wettability/saturation data point for sample 14-7 (Red traces on **Figure 4**). Comparing this partially saturated T_2 spectrum with the the 100% S_o and 100% S_w distributions it is impossible to determine the individual contributions from decane and brine. In fact, the partially saturated distribution looks like the 100% S_w T_2 distribution alone. As a result, the NMR wettability model always predicts that the partially saturated T_2 distribution is entirely composed of the 100% S_w distribution meaning the wettability and brine saturation do not change as the sample imbibes decane. Obviously, this is not accurate and the D_2O data better captures what is occurring within the rock. The green trace in the lower right-hand panel of **Figure 5** shows the T_2 distribution recorded for sample 14-7 while it was 100% D_2O saturated imbibing decane. This distribution, which corresponds to the last data point recorded for decane imbibition of sample 14-7 (Green traces on **Figure 4**), shows only signal from decane within the sample. When comparing the red and green traces in the lower right panel of **Figure 5**, it is clear that some of the partially saturated T_2 distribution is composed of decane. As a result, the prediction of the NMR wettability model that the saturation (and hence wettability) of sample 14-7 is not changing from 100% brine saturated as it imbibes decane is not accurate. Instead, the D_2O data is showing, more logically, that the rock is becoming less brine saturated and hence less water wet as it imbibes decane.

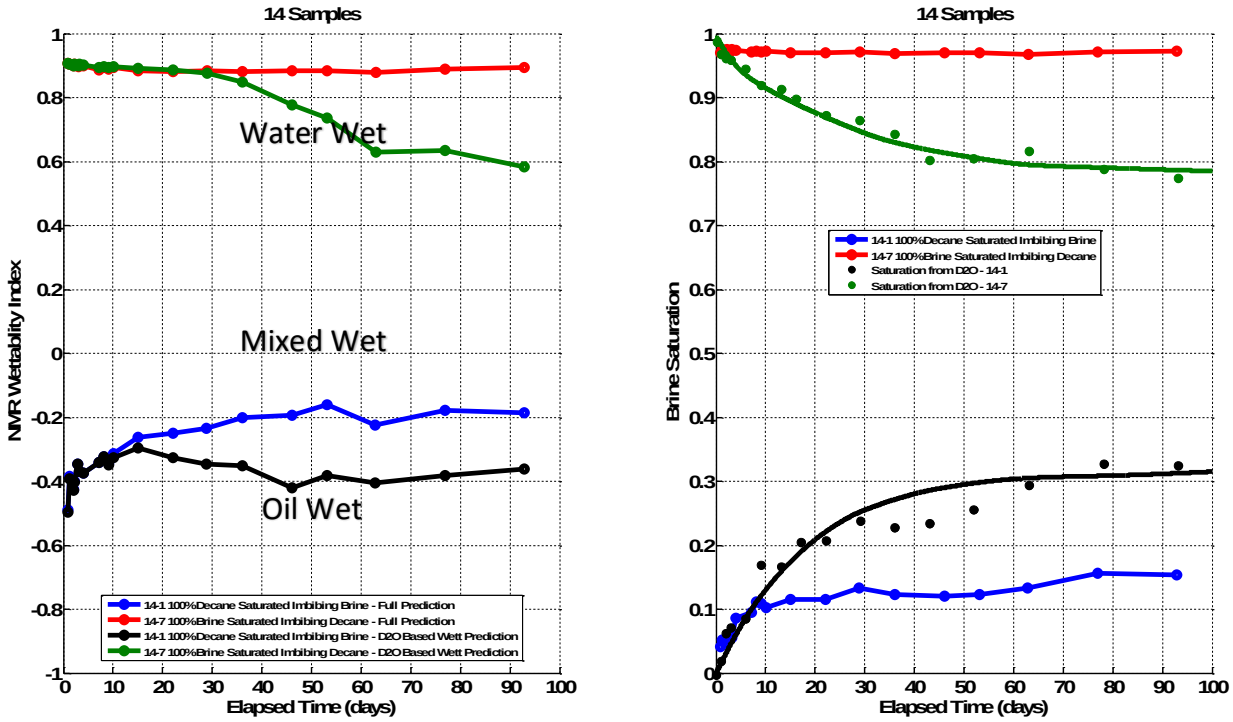

Figure 4: The results of the wettability analyses for twins 14-1 and 14-7 are shown. The left-hand panel shows the wettability as a function of imbibition time for both samples, while the right-hand panel shows the water saturation as a function of imbibition time for both samples.

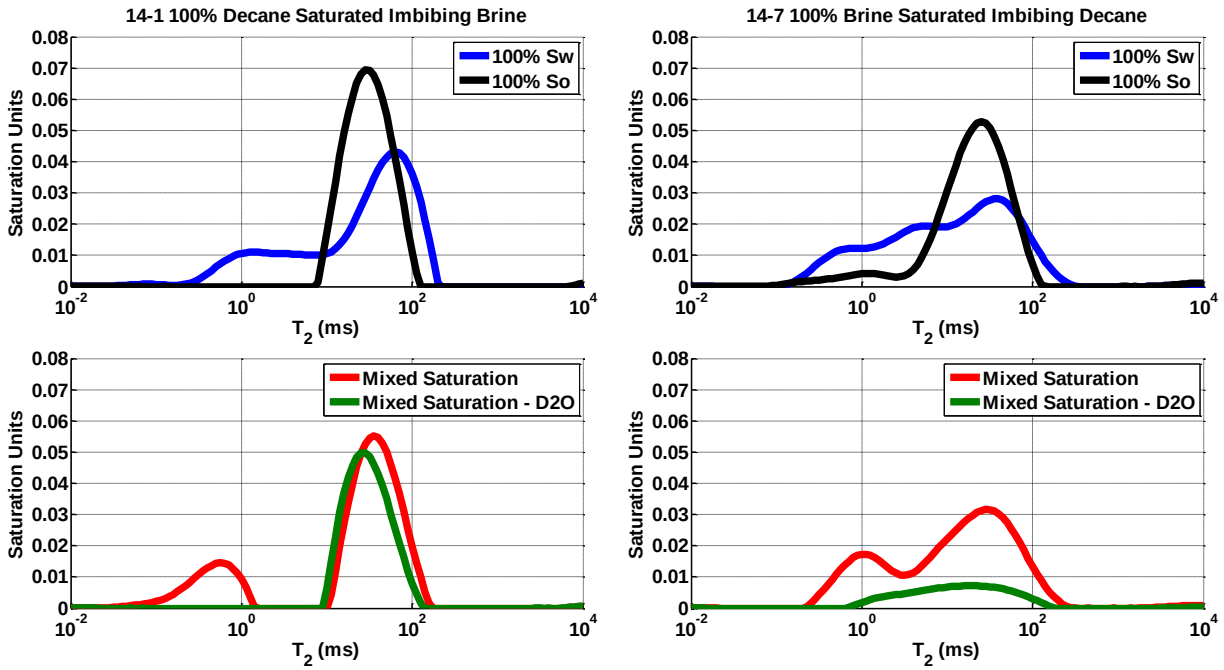

Figure 5: The upper panels are a comparison between the 100% brine saturated (blue trace) and 100% decane saturated (black trace) for samples 14-1 and 14-7. The NMR wettability model mixes these spectra to give a predicted T_2 spectrum which is compared to a T_2 spectrum recorded from a sample partially saturated with both water and oil whose wettability is to be determined (red trace lower panels). The green traces in the lower panels are the T_2 distributions recorded for the partially saturated 14 samples during the D_2O imbibition studies. In these spectra, only signal from decane is observed so subtracting it from the partially saturated T_2 spectrum (red traces) it is easy to determine the brine and decane saturation for this partially saturated data. Without the D_2O the wettability analysis fails as the saturation of the mixed wettability samples cannot be determined accurately.

Again, the wettability predicted when the brine saturation from the D_2O analysis is employed is taken as more accurate than that predicted by the wettability model alone because the brine saturation is determined without ambiguity. Unfortunately, neither the brine saturation or the wettability determined from the D_2O data for samples 14-1 and 14-7 converged in a single wettability region. This offset was perplexing and made it difficult to say definitively whether these samples are water, oil or mixed wet. Upon revisiting of the sample stations, we saw that these samples were plugged with some offset at a transition zone and 14-7 is a more marly rock type and should not be directly compared with its 14-1 counterpart. Ergo, the 14-1 and 14-7 can be considered, respectively, a chalk and a marly-chalk facies of distinct wettability indices.

Further Validation: Mass Balance Analysis

Because the predicted brine saturations and D_2O based saturations differed and fixing the brine saturation to the D_2O data was relied on to retrieve valid NMR wettability indices for samples 14, another method for further validating the brine saturations was investigated. As mentioned earlier, the samples were weighed prior to every NMR measurement. Therefore, the brine saturation of each sample could be determined from mass balance. **Figure 6** compares the brine saturations predicted from the NMR wettability analysis with those determined from the D_2O data and those determined from the mass data for samples 14-1 and 14-7. For sample 14-1, the agreement between the D_2O based brine saturation (**Figure 6** – black trace) and the saturation derived from the mass balance analysis (**Figure 6** – brown trace) is very good. The mass data does have more oscillation in it as compared to the D_2O data. This is a result of the larger error associated with the mass measurements as compared to the D_2O NMR measurements. However, both the mass and D_2O based saturation versus elapsed time plots predict a higher brine saturation than that derived directly from the NMR wettability analysis (**Figure 6** – blue trace). For sample 14-7, both the brine saturation derived from the mass balance analysis (**Figure 6** - purple trace) and the D_2O based saturation data (**Figure 6** – green trace) predicts a saturation lower than the brine saturation derived from

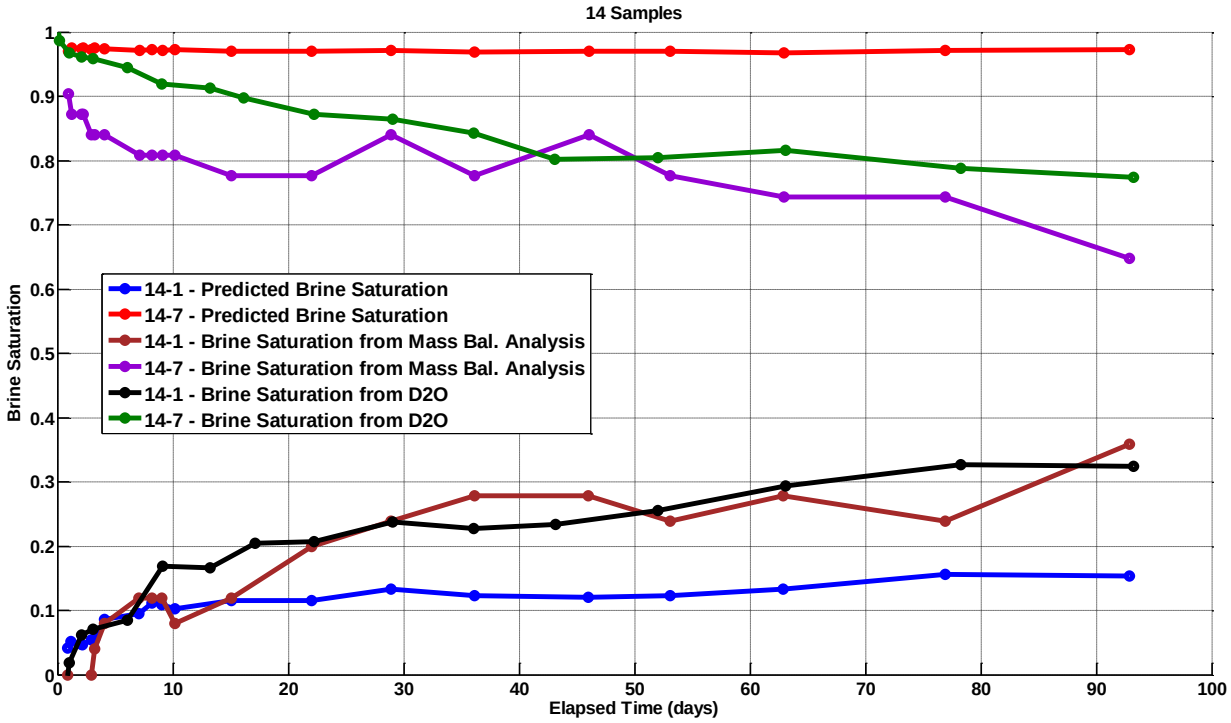

Figure 6: Plot compares the brine saturations predicted from the NMR wettability analysis with those determined from the D_2O data and those determined from the mass data for samples 14-1 and 14-7. In general, the brine saturation predicted by the mass and D_2O data agree very well with each other but differ from the saturation predicted by the wettability analysis alone.

the wettability analysis alone (**Figure 6** – red trace). The good agreement between the mass and D_2O based saturations (similar results also observed for 9 and 12 samples) gave us further confidence in the validity of fixing the saturations at the D_2O data and retrieving the associated wettability.

Further Validation: T_1-T_2 Maps

Another possible way to differentiate between decane and brine contributions to the NMR signal from the core samples is to examine T_1-T_2 maps. These two-dimensional measurements explore differences in molecular self-diffusion of brine and oil in addition to bulk properties and surface interaction (relaxation), providing a way to separate the overlapping NMR signals from the oil and brine within the pores of the sample. **Figure 7** shows the T_1-T_2 maps for the 100% brine saturated, 100% decane saturated and mixed decane/brine saturated states for sample 9-P1A, respectively. The mixed saturation state was achieved by letting the fully decane saturated sample imbibe brine to steady state. Most of the brine and decane signature did, unfortunately, overlap for this sample and all the other samples investigated. For example, the 100% S_w and 100% S_o maps in **Figure 7** are very similar and, consequently, most of the signal from the mixed saturation sample (**Figure 7** – right panel) cannot be conclusively separated in to decane and brine contributions. This is not surprising as decane, a unimolecular light oil, has a viscosity and diffusion coefficient similar to brine. This limited contrast in diffusivity limits the NMR ability to separate oil from brine in small pores, even in T_1-T_2 maps. The only region in the T_1-T_2 maps where we observe a difference between decane and brine is the lower left segment (T_1<10 ms and T_2< 1 ms), which represents fluids contained in the smallest pores. For the 100% S_w map (**Figure 7** – left map), there is clearly signal originating in the smallest pores while for the 100% S_o map (**Figure 7** – middle map) there is no signal in this lower left segment. One potential interpretation is that the smallest pores are void of liquid for the 100% S_o sample, but we know this is not the case because the measured NMR volume is identical in each T_1-T_2 map. Given that decane has a diffusion coefficient similar to brine, **Figure 7** left and middle panels are best explained in terms of wettability: decane enters these smallest pores but does not interact with the pore surface. Consequently, decane does not relax at a comparable rate to brine in these pores and T_2 and T_1 are longer, leaving the lower-left corner in the T_1-T_2 map empty. These differences in the 100%

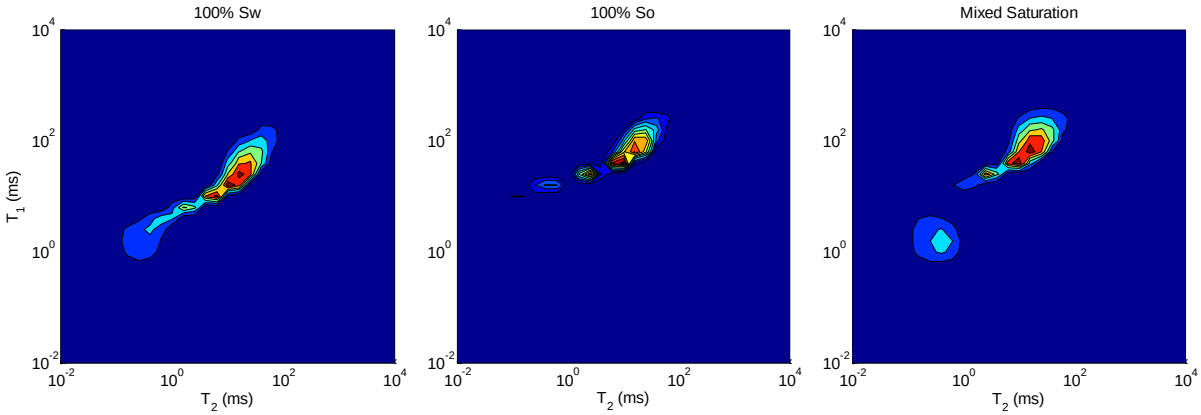

Figure 7: Left to right, T_1-T_2 maps for the 100% brine saturated, 100% decane saturated and mixed decane/brine saturated states for sample 9-P1A . Mixed saturation state was reached by letting the100% decane saturated imbibe brine for over ninety days.. NMR volume is the same in all maps. It can be inferred that smallest pores of the mixed saturation sample are filled with water and are water wet: oil does not relax at the surface of these small(est) pores and consequently, T1 and T2 are longer, leaving the lower-left corner of the map void of signal.

S_o vs 100% S_w maps are instrumental to the interpretation of which pores are decane-filled and which pores are water-filled in the mixed saturation sample. The T_1-T_2 map for the mixed saturation sample shown in right panel of **Figure 7** features signal amplitude in this lower left corner of the map, which implies that the smallest pores of the mixed saturation sample contain water and are water wet. Segmentation of the T_1-T_2 maps for the mixed saturation state sample shows that about 1/3 of the measured fluid volume is contained within these smallest pores. This analysis is consistent with T_1-T_2 ratio analysis in which different fluids can be assigned different T_1-T_2 ratios (Kausik et al., 2016). T_1-T_2 ratio for water is one so the water signal is found close to the diagonal in the T_1-T_2 map. The NMR wettability analysis indicates the overall steady-state wettability of sample 9-P1A after ninety days of brine imbibition is -0.2. Therefore, if these smallest pores are indeed water wet, then the larger pores have to be neutral/intermediate to oil wet in order to yield and explain an overall mixed wettability for sample 9-P1A; more discussion on this in the subsequent section. Overall, while the T_1-T_2 maps failed to determine brine/decane saturations, they did offer insight on the relative wettability of different sized pore networks.

DISCUSSION

Table 4 collates the results from this study and previous work (Kelly et al., 2020) to facilitate practical interpretations from the varied spontaneous imbibition trends. In this interpretation section we refer to decane as "oil" and brine or D_2O as "brine" to generalize the displacement results for upscaling interpretations. The results rows in **Table 4** are ordered from smallest (most oil wet) to largest (most water wet) NWI for each displacement type. For **brine-displacing-oil**, the results show that the more oil wet the sample is on the NWI spectrum the lower the steady state Sw-value (less oil displaced). Correspondingly, for **oil-displacing-brine**, the more water wet the sample is on the NWI spectrum the greater the steady state Sw-value (less brine displaced). Both trends align with expectations. The exception to the trends are the 2-P chalk samples from Reservoir B, shown to be the highest water-wet NWI of all the sample sets, yet, demonstrating considerable displacement by decane. These samples contain minimal organic matter (see **Table 1**) which supports the highly water wet NWI value, though organic matter content is not a wholly determining wettability factor. The results are also shown in terms of bulk volume water (BVW) or bulk volume hydrocarbon (BVH) remaining, which factors in the different sample porosity values to assist with comparability among reservoirs.

Insights from Time-Lapse NWI Experiments

The duration of the imbibition process to reach steady state and saturation (S_w) at steady state are summarized in **Table 4** and can be used to interpret the relative wettability of different-sized pore networks, as illustrated in the examples in the following paragraphs. A primary observation is that except for the siltstone GP2/GP3 sample set, *none* of the studied sets of twin samples reached the same steady state S_w values in their respective displacements. We attribute this offset to the

Table 4: Core Plug Sample Steady-State NMR Saturations and Wettability Indices

Sample Information				Steady State				Wettability**	
Reservoir ID	Sample Name	Invading Fluid	Defending Fluid	Time (days)	Sw (approx.)	PHI (p.u.)	BVH or BVW remaining	Steady-State NWI	D_2O vs. Brine Validation Match
Brine-displacing-oil - spontaneous imbibition									
A	7-P3A	Brine	Decane	120	25%	12.5	9%	-0.55 Oil wet	Good to fair
D	14-1	Brine	Decane	60	30%	7.2	5%	-0.35 Slightly oil wet	Discrepancy; use D_2O as primary
A	9-P1A	Brine	Decane	30-45	35%	10.3	7%	-0.2 Mixed wet	Good to fair
C	GP3	Brine	Decane	20	45%	8.8	5%	0.35 Slightly water wet	Good to fair
B	2-P1A	Brine	Decane	50	40%	4.3	3%	0.9 Highly water wet	Good to fair
D	12-1*	Brine	Decane	--	--	6.3	--	--	--
Oil-displacing-brine - spontaneous imbibition									
A	7-P2	Decane	Brine	120	10%	12.5	1%	-0.5 Oil wet	Good to fair
C	GP2	Decane	Brine	90	45%	8.8	5%	0.25 Mixed wet	Good to fair
A	9-P3	Decane	Brine	30-45	65%	10.3	7%	0.3 Mixed wet	Good to fair
D	12-6	Decane	Brine	50	75%	4.6	3%	0.4 Slightly water wet	Discrepancy; use D_2O as primary
D	14-7 +	Decane	Brine	60	80%	6.6	5%	0.6 Water wet	Discrepancy; use D_2O as primary
B	2-P2	Decane	Brine	120	15%	4.3	1%	0.9 Highly water wet	Good to fair

* Sample parted during experiment.
\+ Sampling offset at a transition zone; upon inspection, 14-7 is a more marly rock type and should not be directly compared with its 14-1 counterpart.

low connectivity and local heterogeneity characteristic of UR rocks. For a well-connected media, generally the same pores that are invaded with nonwetting liquid during forced imbibition (the pressure saturation step in our experiment) spontaneously imbibe the available wetting liquid when exposed to it and reach approximately the same steady state S_w in either displacement direction; one can imagine a bundle of capillary tubes model of different sizes and wettabilities to cleanly visualize this displacement. Another key observation is that many of the samples are characterized to have mixed-wet NWI values, two example interpretations of corresponding wetting distribution discussed below.[3]

As an end-member case, mixed wettability can be interpreted as independent wetting systems/surfaces of varying fractions of distinctly different wettability values. For example, in the siltstone GP2/GP3 sample set (NWI = 0.25-0.35, mixed wet), brine-displacing oil imbibition occurred at a rate more than four times faster than oil-displacing-brine imbibition, but both cases ultimately ended at the same steady state S_w. This trend suggests that the water wet pore surfaces are generally associated with larger pores, as per the classic Washburn

[3] Note that the mixed-wet interpretation examples are non-unique. Inherent heterogeneity between sample "twins" and potential differences in the magnitude of contact angles between different fluid-rock surfaces within the core plugs (i.e., pore size is not the only control on imbibition rate) are factors as well and the interpretation robustness benefits from integrating with other data, including petrography.

(1921) equation for imbibition, for with all other properties roughly consistent, imbibition occurs faster in larger pores. Hence, the time-lapse wettability analysis suggests that the siltstone sample is likely composed of dual pore system with distinctly different wettability, with the larger pores being water wet (most likely inter-crystalline pores). In addition, both pore- networks are adequately connected that they can each be accessed through spontaneous imbibition alone.

For another distinct end-member case, mixed wettability can be interpreted as local surfaces having an affinity for both brine and oil or being neutral/intermediate wetting (muted contact angles, lacking a strong wetting preference). For example, the NWI values for the 9-P high-maturity marl samples (NWI = -0.20 and 0.30, mixed wet) suggest an increase in neutral to water wetness with maturity when compared to the 7-P low-maturity marl samples from the same reservoir unit (NWI = -0.55, oil wet) with similar clay content, porosity, and organic content TOC (see **Table 1**). This finding aligns with literature reports that organic matter wettability changes with the maturity-driven number of surface functionalized (polar) sites, which can be locally heterogenous; the molecular dynamics work of Hu et al. (Hu et al., 2016) summarizes this topic and related experimental findings. The 9-P steady-state NWI values, though both in the mixed-wet regime, differed notably between brine-displacing-oil imbibition (-0.2) and oil-displacing-brine imbibition (0.3). Furthermore, the same pore volume (S_w or S_o = ~35%) was displaced at the same rate (30-45 days) for the 9-P brine-displacing-oil and oil-displacing-brine experiments, suggesting that similar pore sizes are invaded in both cases and that at least one third of the 9-P pore volume is not accessed with spontaneous imbibition of either liquid. This behavior is in stark contrast to the imbibition characteristics of the 7-P low-maturity marl samples where the entire pore volume was eventually accessed via spontaneous imbibition. Further, the T_1-T_2 maps in **Figure 7** suggest that 1/3 of the 9-P pore volume is housed in the smallest pores, in alignment with the displaced pore volume in both imbibition experiments; the previous section explained that the pores in that segment are likely water wet. Overall, one potential interpretation based on the above discussion is that some of the 9-P pore system is generally harder to access with capillary forces alone (spontaneous imbibition) due to neutral/intermediate contact angles at those surfaces.

Given enough soak time (order of weeks in this study), the level of spontaneous saturation change in some of these tight rock plugs is impressive; for example, in 7-P2 and 2-P2, spontaneous imbibition alone was akin to bring the rocks to an approximate S_{wi} value for oil-displacing-brine. In the chalk 2-P samples, brine-displacing-oil into a water wet system (NWI = 0.9) occurred ~2.5 times faster than the "off-trend" oil-displacing-brine case, suggesting the decane flow was relegated to either smaller pores and/or pores with wetting films of water, the latter a more reasonable hypothesis based on the NWI and saturation results. The actuation mechanism for oil-displacing-brine spontaneous imbibition in the 2-P samples is still a subject of investigation. We recommend applying the NWI methodology to forced imbibition experiments with multiple pore volumes, if possible, to better quantify steady-state *residual* saturation values.

Based on this discussion, one can surmise why it is especially important to quantify wettability state in UR rocks: whether brine-displacing-oil (waterflooding or hydraulic fracturing scenario) or oil-displacing-brine (flowback from reservoir into the invaded fracture-matrix interface zone), wettability (or lack thereof in neutral wet cases) typically dictates transport in inherently tight and complex pore systems. If an operator believes imbibition is a major production driver then more water-wet results are favored. However, if an operator is concerned about mitigating relative permeability issues at this interface, then more oil-wet results are favored; classically, oil-wet samples have lower residual oil saturation (S_{or}), as connectivity of a wetting phase is maintained by film layers and/or smaller (and relatively isolated) pores holding the wetting phase. The discrete NWI/saturations result values may differ when lab oils or crude oil are used or different sample preservation and preparation methods applied, all assessments that can be subjects of future applications of NWI. However, the observations this workflow enables with respect to interpreting the wettability state of a sample and the relative wettability of different-sized pore networks are salient.

Comparison with Other NMR Wettability Methods

As mentioned earlier, we employ the Looyestijn method for determining the NMR based wettability index. Looyestijn's work was entirely based on conventional samples. We have extended the application for the model in a sense that we apply it to unconventional samples (Dick et al., 2019; Kelly et al., 2020) and continue that work in this paper. The main differences in conventional vs. unconventional samples are that T_2 relaxation in

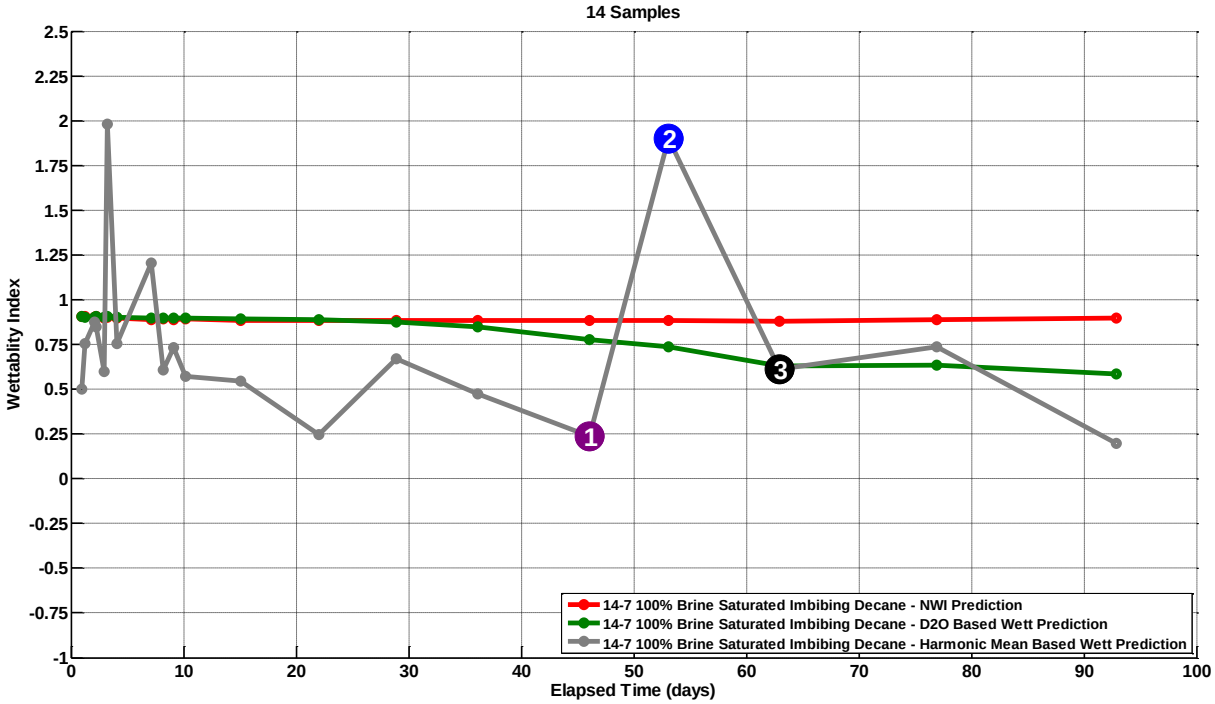

Figure 8: The wettability derived from the harmonic mean-based wettability data (I_{HM}) vs elapsed time (gray trace) is plotted for sample 14-7. Also shown are the NWI calculated using NWI (red trace) and the D2O based wettability (green trace). The median value for the harmonic mean-based wettability vs. elapsed time data is about 0.5 or slightly water wet. What is lost in the harmonic mean-based wettability data is any trend in the wettability as a function of time. This is due to the large oscillations in the data, including some points where the wettability index exceeds the allowed value of +1.

unconventionals is usually much shorter and that organics and organic hosted pores are present in unconventionals. These make the analysis more challenging because organic and non-organic hosted pores could have different wettabilities within the same sample so what we end up measuring is the average wettability. Another challenge is that T_2 distributions of 100% decane saturated sample and 100% brine saturated sample often have a high degree of overlap, making it difficult for the model to distinguish between the two.

We compared our wettability results with other NMR-based models and show the comparison of our results with those of Tandon et al. (2017) herein. Their model is the most like our approach in that it can be applied to any partially saturated mixed wettability rock, does not employ measurement at S_{wi} or S_{or} and does not rely solely on peak positions making it more suited to multimodal T_2 distributions. Their wettability index (I_{HM}) is then calculated with the harmonic mean employing the following equation.

$$I_{HM} = \frac{2\left(\frac{1}{T_{2HM}}-\frac{1}{T_{BHM}}\right)-\left(\left(\frac{1}{T_{2WHM}}-\frac{1}{T_{BW}}\right)+\left(\frac{1}{T_{2OHM}}-\frac{1}{T_{BO}}\right)\right)}{\left(\frac{1}{T_{2WHM}}-\frac{1}{T_{BW}}\right)-\left(\frac{1}{T_{2OHM}}-\frac{1}{T_{BO}}\right)} \quad (6)$$

T_{2HM} is the harmonic mean of the T_2 distribution of the partially saturated mixed-wet sample, T_{2WHM} is the harmonic mean of the T_2 distribution of the 100% S_w sample, T_{2OHM} is the harmonic mean of the T_2 distribuiton of the 100% So sample, T_{BO} is the harmonic mean of the T_2 distribution of bulk decane, T_{BW} is the harmonic mean of the T_2 distribution of bulk brine and T_{BHM} is the harmonic mean of the bulk decane and brine T_2 distributions mixed. As can be seen, from equation (6) the Tandon et al. wettability model employs the same T_2 distributions as our approach (i.e. 100% S_o, 100% S_w, bulk decane and bulk brine). The central difference between their model and our approach is that they do not rely on a fit of the entire T_2 distribution but rather calculate the harmonic mean of each distribution.

Figure 8 shows the I_{HM} vs elapsed time (gray trace) for sample 14-7. Also shown are the NWI calculated using our approach (red trace) and the D_2O based wettability (green trace), previously plotted in **Figure 4**. From **Figure 8**, you can see that the median value for the harmonic mean-based wettability vs. elapsed time data is about 0.5 or slightly water wet. What is lost in the harmonic mean-based wettability data is any trend in the wettability as a function of time. This is due to the large

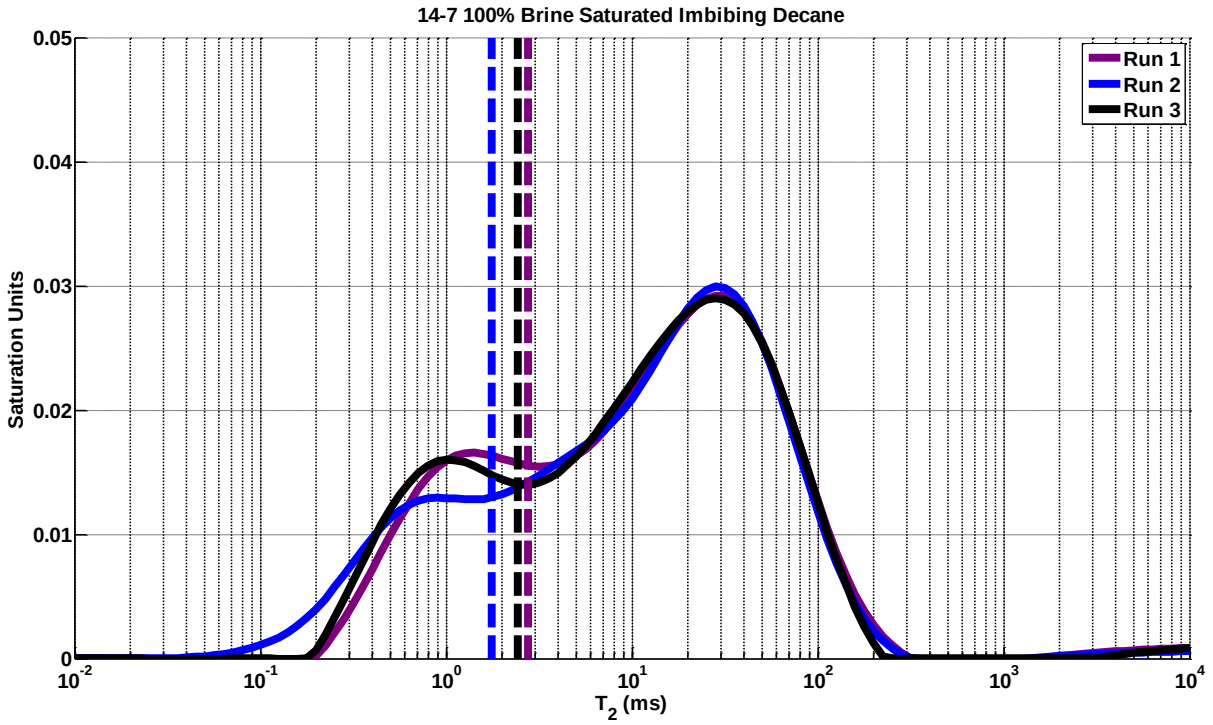

Figure 8: The T_2 distributions for sample 14-7 from data points 1, 2 and 3 in Figure 7. The dashed lines are the harmonic means for runs 1, 2 and 3. There are small differences in the distributions at the lower T_2 values. These differences lead to differences in the harmonic mean of each distribution which can further lead to large differences in the wettability derived from the harmonic mean.

oscillations in the data, including some points where the wettability index exceeds the allowed value of +1.

Equation 6 shows that for the same mixed wettability sample whose wettability is changing over time, the I_{HM} is determined entirely by the $\left(\frac{1}{T_{2HM}} - \frac{1}{T_{BHM}}\right)$ term. The other terms in the equation are determined by the 100% S_w, 100% S_o, bulk brine and bulk decane T_2 distributions which are invariant for a fixed sample. In addition, because the bulk brine and decane T_2 distributions occur at much higher values than the distributions for the mixed wettability sample, the $\frac{1}{T_{BHM}}$ will be significantly smaller (near zero) compared to the $\frac{1}{T_{2HM}}$ term and can be neglected in the determination of I_{HM}. In other words, only the T_2 distribution of the mixed wettability sample needs to be considered when comparing wettability for the same sample. **Figure 9** shows the T_2 distributions for sample 14-7 from data points 1, 2 and 3 in **Figure 8**. At first glance, the T_2 distributions in **Figure 9** are very similar. However, there are small differences in the distributions at the shorter T_2 values corresponding to the smallest pores. For example, run 2 has some porosity below 0.15 ms whereas runs 1 and 3 have no porosity below 0.15 ms. While the contribution to run 2 by porosity at the lowest T_2 values does not seem like a significant contribution to the overall T_2 distribution it is enough to push T_{2HM} value for the distribution lower. For example, the harmonic mean for the distribution for run 2 is 1.75 ms (**Figure 9** – dashed blue line) while the harmonic mean for run 3 (**Figure 9** – dashed purple line) is 2.75 ms. This does not seem like a large change in the harmonic mean, but it is significant because of the relative values of each of the terms in Equation 6 and the fact that I_{HM} is inversely proportional to T_{2HM}. Both of which can result in small changes in harmonic mean leading to large changes in I_{HM}. This is reflected in the large variability of the harmonic mean-based wettability data plotted in **Figure 7** (gray trace).

Small changes in T_2 distributions are common and can be caused by real difference in the observed porosity distributions as the wettability changes or can be the result of experimental error (including differences in the signal to noise ratio) in the NMR data from which the T_2 distributions are derived. The Looyestijn method is less susceptible to these small discrepancies leading to large variances of the calculated NWI because it uses the

whole T_2 spectrum. This makes it more suitable for data sets like the ones studied in this paper, where oil and water T_2 spectra are complex with multiple peaks. This is reflected in the more stable NWI vs time data for sample 14-7 (**Figure 8** – red trace). In addition, because the Looyestijn method also provides saturation data as part of its output, it gives an independent method for verification of the results using D_2O data (**Figure 8** – green trace). The other samples (Samples 12 and 9-P) we studied showed similar variability of the harmonic mean-based wettability results.

The original intent of the D_2O imbibition experiments was only to validate the results of the wettability analysis. However, this study revealed that for some samples, especially those of smaller pore volume (a few percent, see **Table 4**), there is disagreement between the brine saturations derived from our wettability analysis as compared the D_2O data. We have shown that an analyst can fix the saturations at the D_2O value and reevaluate the wettability, or, for less ambiguity, apply the D_2O saturation/wettability analysis as the primary method of determining the wettability index from NMR data.

Finally, this work applied considerable effort towards validating the results of the presented wettability analysis, confirming the brine saturations derived from our wettability analysis with those determined independently via both mass and repeated D_2O data. In addition, we have shown that our method is more robust and well suited for determining the wettability of unconventional samples as compared to other NMR methods, due the challenging spectra inherent with unconventional samples. To our knowledge, this study is the most robust validation of an NMR wettability analysis on unconventionals done to date, enabling confidence in the results and method.

CONCLUSIONS

We adapted the NMR-based wettability index (NWI) methodology of Looyestijn et al. (2006) and applied to unconventional rocks. We utilized the index in a time-lapse imbibition data workflow and, following extensive validation, discussed how the results can be interpreted for practical application. Our method was applied to a variety of rock types and formations to test its robustness and learn about the wettability variation of major North America unconventional plays. We found that the NWI model implemented is well suited for data sets featuring complex oil and water T_2 spectra with multiple peaks, but that for especially challenging samples D_2O should be used in addition to brine, providing robust, non-ambiguous results. In addition, we show that our method, which utilizes full T_2 spectra, outperforms single T_2 value-based models, producing more stable results; minor variations in T_2 spectra do not cause major swings in the NWI result. Finally, this wettability quantification method is especially relevant to the fluid-rock interaction challenges facing unconventional operators today: consistent wettability characterization can guide technical decisions related to fracture fluid additives and soaking times and bound the relative permeability curves selections used in reservoir modeling of matrix-fracture interface regions.

ACKNOWLEDGEMENTS

The authors thank ConocoPhillips Company for support of this work and to company business unit partners for contributing samples towards the wettability study. We also thank Green Imaging Technologies and H2 Laboratories for instrument time and NMR data acquisition and analysis.

REFERENCES

Dick, M.J., Veselinovic, D., Green, D., Scheffer-Villarreal, A., Bonnie, R.J.M., Kelly, S. and Bower, K. "NMR Wettability Index Measurements on Unconventional Samples", Unconventional Resources Technology Conference, Denver, CO, USA, 22-24 July 2019.

Fleury, M. and Deflandre, F., "Quantitative evaluation of porous media wettability using NMR relaxometry", Magnetic Resonance Imaging (2003), **21**, 385-387.

Hirasaki, G. J. (1991, June 1). "Wettability: Fundamentals and Surface Forces", Society of Petroleum Engineers. doi:10.2118/17367-PA.

Howard, J.J., "Quantitative estimates of porous media wettability from proton NMR measurements", Magnetic Resonance Imaging (1998), **16**, 529-533.

Hu, Y., Devegowda, D., Sigal, R. "A microscopic characterization of wettability in shale kerogen with varying maturity levels", Journal of Natural Gas Science and Engineering (2016), **33**, pages 1078-1086.

Kausik, R., Fellah, K., Rylander, E., Singer, P. M., Lewis, R. E., Sinclair, S. M. "NMR Relaxometry in Shale and Implications for Logging." Petrophysics 57 (2016): 339–350.

Kelly, S., Bonnie, R.J.M., Dick, M.J., Veselinovic, D., . "NMR Time-Lapse Wettability Assessments in Unconventional: Insights from Imbibition", Unconventional Resources Technology Conference,

Houston, TX, USA, 20-22 July 2020.

Looyestijn, W.J. and Hofman, J.P., "Wettability Index Determination by Nuclear Magnetic Resonance", SPE 93624, presented at the MEOS, Bahrain, March 2005. Published in SPEREE April 2006, pp 146 – 153.

Looyestijn, W., Zhang, X., and Hebing, A., "How can NMR assess the wettability of a chalk reservoir", Society of Core Analysts, Vienna, Austria, 27 August-1 September 2017.

Morrow, N. R., Ma, S., Zhou, X., & Zhang, X. (1994, January 1). "Characterization of Wettability From Spontaneous Imbibition Measurements", Petroleum Society of Canada. doi:10.2118/94-47.

Newgord, C., Tandon, S., Rostami, A., and Heidari, Z. "Wettability quantification in mixed-wet rocks using a new NMR-based method: experimental model verification", (SPE-191509-MS), Society of Petroleum Engineers Annual Technical Conference and Exhibition, Dallas, TX, USA, 24-26 September 2018.

Tandon, S., Rostami, A., and Heidari, Z. "A new NMR-based method for Wettability Assessment in mixed wet rocks", (SPE-187373-MS), Society of Petroleum Engineers Annual Technical Conference and Exhibition, San Antonio, TX, USA, 9-11 October 2017.

Washburn, E. W., "The Dynamics of Capillary Flow", Physical Review (1921), **17**, issue 3, pages 273-283.

ABOUT THE AUTHORS

Shaina Kelly is a petrophysicist/engineer specializing in fluid flow and transport in porous media characterization and special core analysis. Shaina joined ConocoPhillips (Geoscience organization) as a Senior Petrophysicist in 2016 and has worked on core and log analysis for various Lower 48 and international conventional and unconventional plays. Shaina has a Bachelor of Science in Environmental Engineering from the University of Florida and Master's and PhD degrees in Petroleum Engineering from The University of Texas at Austin. She is technical leader in nanoscale transport studies and pore-scale and fluid-rock interaction research programs, with 10+ related publications. When not studying rocks, Shaina enjoys endurance sports and reading.

Ron J.M. Bonnie joined ConocoPhillips in 2010 as Petrophysical Advisor in the Geoscience organization. Before, Ron has worked more than 15 years for Shell E&P in The Netherlands and Houston in a multitude of assignments in research, petrophysics, geophysics and operations. He was also 6+ years with Halliburton in the USA with positions in R&D for Numar and as Global Product Champion MRILWD for Sperry-Sun. Ron is an industry-expert on NMR technology and provides support for high-profile NMR projects in ConocoPhillips globally plus guidance, support and evaluation of petrophysically challenging projects in traditional and unconventional reservoirs. Ron is very well published and holder of several patents. He has a B.Sc. and M.Sc. in nuclear physics from the University of Amsterdam and a Ph.D. in laser physics from Twente University (both in The Netherlands). Ron is an avid long-distance runner and motorcyclist.

Mike Dick has a Bachelor of Science degree from the University of New Brunswick. His post-graduate work focused primarily on molecular physics and included both a Master's degree from the University of New Brunswick and a Ph.D. from the University of Waterloo. After graduation, Mike's career diversified working first in astrophysics while doing a post-doctoral fellowship at NASA's Jet Propulsion Lab. Following this position, Mike moved into the field of nuclear physics in Chalk River Ontario with Bubble Technology Industries (BTI) as a research scientist. His work with BTI focused primarily on developing unique radiation detectors for defense and homeland security organizations, first responders, space agencies, regulatory/standards groups, and research institutions. This work has resulted in three patent filings. Mike joined the Green Imaging Technologies in September 2015 as a Principal Research Scientist. Mike works closely with our research team innovating new NMR techniques and tools for our clients.

Dragan Veselinovic is the Senior Applications Specialist for Green Imaging Technologies. He holds a Master's of Science in Physics degree from the University of New Brunswick. He has worked in several capacities at GIT, which has allowed him to become the "Go To" person for GIT customers. Dragan conducts research, manages the laboratory, and trains all new customers. He also plays an important role in many of the research and development projects undertaken by GIT.